Investigation of Surface Layer and Wear Behavior of Nitrided Gear Drives

Claus Razim, Mercedes Benz AG
Stuttgart, Germany

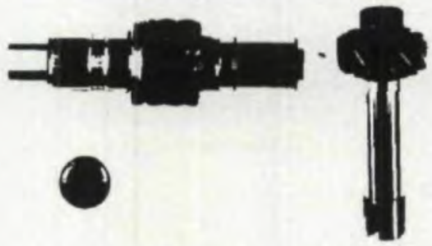

	Intermediate Gear	Helical Gear
Standard Treatment	driving gear C15 BNT	driven gear C15 BNT
No. of Teeth	9	12
Max Speed	4300 rpm	3250 rpm
Sliding Velocity	approx 1.6 m/sec at 1000 rpm	
Theoretical Surface Pressure Load	3250 — 4600 N/mm^2 at 1000 rpm	
Power Transmitted	4.3 kW (5.9 PS) max.	

Fig. 1 — Investigated pair of gears.

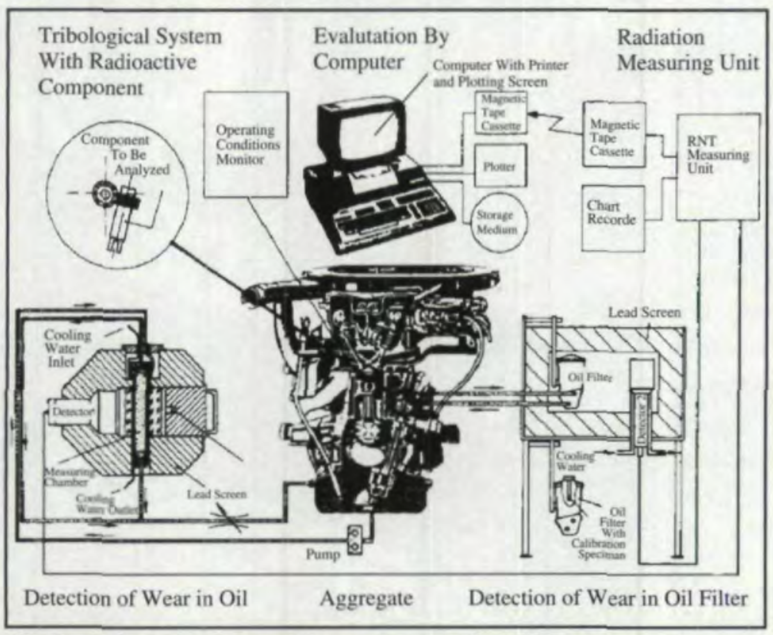

Fig. 2 — Wear measurement by means of radionuclide technology.

In this article we will characterize the nitride layers that are generated by different nitriding processes and compare their respective wear characteristics.

Test Apparatus

Fig. 1 shows a pair of gears on which the wear measurements were carried out: an intermediate gear and a helical gear, which drive the oil pump of a combustion engine. These gears were nitrided by different methods. Fig. 1 also gives some typical data on the gears in question. The components have a high sliding velocity and a very high theoretical surface load. The wear of the helical gear used here has been measured by means of radionuclei technology (RNT). In the process not less than two helical gears ready for installation were activated by neutron radiation. The wear particles of such a radioactive gear can be measured very accurately by measuring its gamma radiation and converting it into wear rates, following previous calibration.

Fig. 2 shows the working setup of the RNT measuring apparatus. In this test, a crankcase containing an oil pump and helical gear drive was set up. An individual oil pump was used in place of a complete engine. The intermediate gear shaft is driven directly by a D.C. motor. The load on the system is controlled by varying the diameter of the oil supply line. Speed and oil temperature can also be controlled. If the helical gear develops wear during the test run, the radioactive wear particles pass into the lubrication oil circuit. Some particles are deposited in the oil filter and some are retained in the oil. The amount of wear is measured by two detectors; one in the oil and one in the filter. The total wear is the sum of the two amounts so measured.

Test Program

Fig. 3 shows the test program. The top of the illustration shows the speed of the test, the load of the gears and the temperature. The lower part of the chart shows the test program and the typical wear curves. The test program is composed of three main parts:

a. A "run-in," that is, the first step at the beginning of the curve;

b. The "main run," going up to 94 hours; and

c. The "overload run" of over 21 hours.

The three parameters controlled were speed, load and oil temperature. The test program was selected so that a standard helical gear would only just survive, and that a distinct separation of the good from the bad helical gear sets could be expected. The main parts of the test program are generally reflected in a typical wear curve. Following a rapid rise during the "run-in" at the beginning of the test, only gradual increases will result during the "main run" and the curve will flatten. However, during the overload run, wear will sometimes rise catastrophically. Even though the wear particles in the oil decrease because of the filtering system, the sum of the amounts of wear particles increases. A number of different gears, 6 nitrided by different processes, were subjected to the test program.

Table 1 lists the treatment methods that have been analyzed. These include six bath nitride processes (BNT), five short cycle gas nitriding processes (KNT) and three plasma nitriding processes (PNT) of different manufacturers. Steel C15, identical to SAE 1015, was exclusively used as a basic material. In addition, the wear characteristics of gear sets made of case hardened steel (E) with carbon content of 0.16 and chromium content and manganese content of approximately 1% and lower were measured for comparison. Metallographic examinations were performed on all variants.

(Figs. 4, 4A) The thickness of the compound layer was 18 ± 4 micrometers. The porosity, the diffusion zone, the structure, the microhardness gradient and the measurement of surface roughness were recorded as criteria of the test or service condition. No correlation was established between hardness, surface roughness or wear characteristics. A specific amount of wear can be correlated to each part of the test; that is "run-in," "main run" and "overload run." Total wear was determined by checking residue in the oil and in the filter. However, the total wear is not the only decisive factor; the wear rate must also be considered. It is possible to compare different treatment methods by comparing the amount of wear and wear rates at the same point in time. To make this comparison possible, a representative total wear curve is given for each variant.

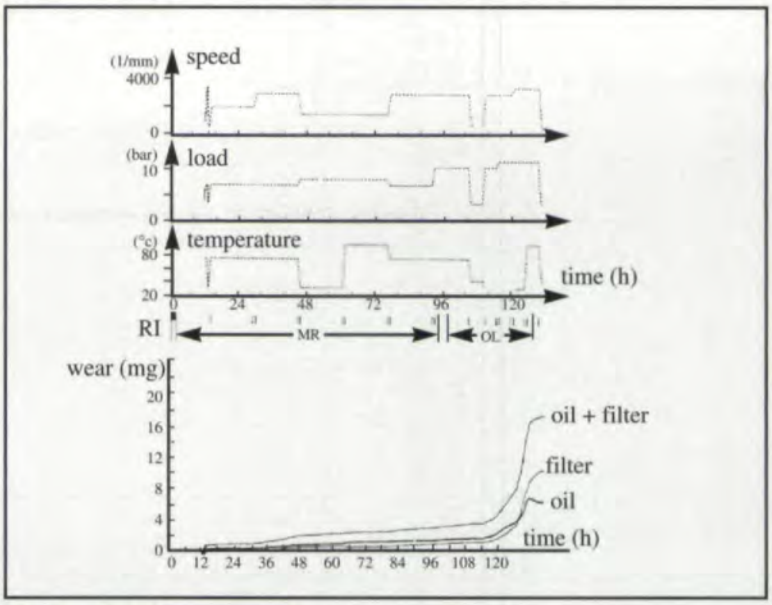

Fig. 3 — Test program and wear curve.

Table 1 — Treatment Variants

No.	Treatment		Material
1	BNT	Salt bath high in cyanide/water	C 15
2	BNT	Salt bath low in cyanide /water	C 15
3	BNT	Salt bath low in cyanide /cooling bath 310° C	C 15
4	BNT	Salt bath low in cyanide /nitriding temperature 610° C	C 15
5	KNT	1.NH3 + exogas 2.NH3 + endogas	C 15
6	KNT	NH3 + methylamine	C 15
7	KNT	NH3 + exogas	C 15
8	KNT	NH3 + endogas	C 15
11	KNT	NH3 + exogas	C 15
12	BNT	Salt bath low in cyanide/water	C 15
9	PNT	Mixed phase	C 15
10	PNT	Monophase γ'	C 15
2/3	PNT	Mixed phase	C 15
2/5	BNT	Salt bath low in cyanide with some ppm S addition	C 15
2/4	E	Case-hardened	16MnCr5

Prof. Dr.-Eng. Claus Razim

is Senior Vice President of Technology and Environment and Chief Enviornment Officer for Mercedes-Benz AG in Stuttgart.

- Determination of Thickness of
  - Compound Layer CL
  - Porosity P
  - Diffusion Zone DZ

  aim CL 18 ± 4 µm
  with PNT variants CL 7-12 µm only

- Structure

- Progression of hardness HV.5 in DZ

- Measurement of surface roughness
  R_a, R_z, R_{3z}

Fig. 4 — Metallographic examinations.

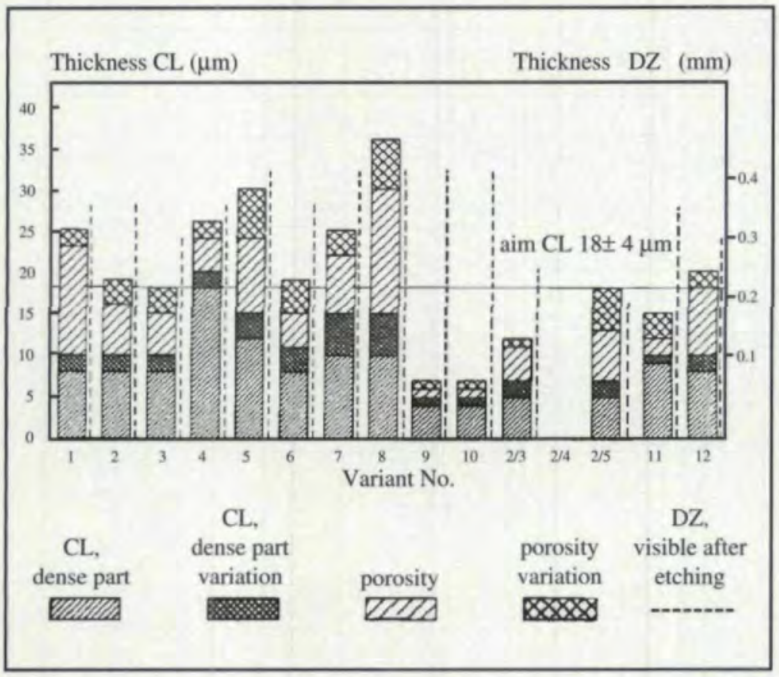

Fig. 4a — Comparison of variants' compound layer, porosity and diffusion zone.

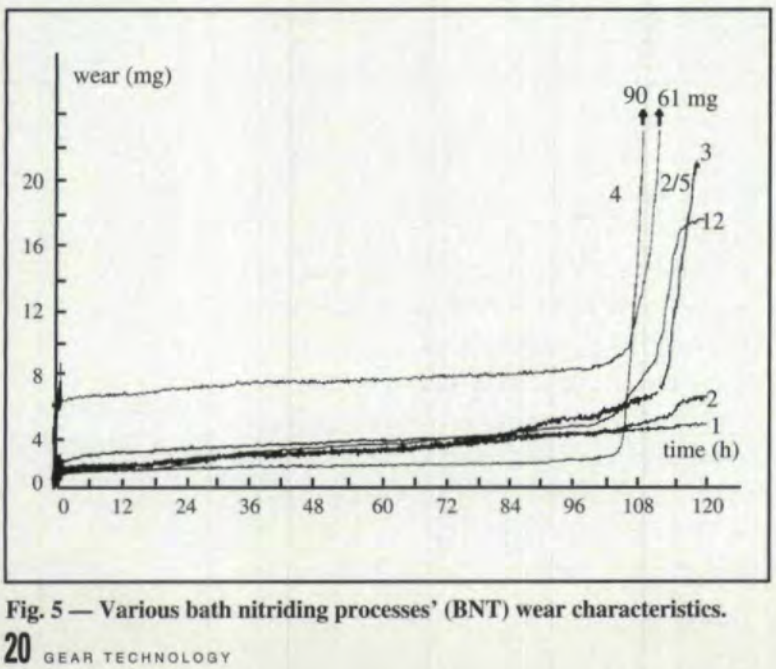

Fig. 5 — Various bath nitriding processes' (BNT) wear characteristics.

Test Results

Fig. 5 shows the curves for all the BNT processes. Up to the end of the main run the wear rates of all variants, with the exception of 2/5 (which has some added sulphur), are within a very narrow range. Only the overload reveals a distinct difference. Variant 1 is the only variant that shows no increased wear during the overload; all other BNT variants have a higher wear rate during this period. The layer developed with the addition of sulphur (2/5) has a high run-in wear and a steep rise in wear during the overload run, but shows an acceptable wear rate during the main run. If we classify the loading to the end of the main run as being medium, all BNT layers over this range are approximately on the same level. For high loads, as in the overload run, the layer developed in the salt bath that was high in cyanide/water (shows the best results).

Fig. 6 shows the least favorable curves for short cycle gas nitrided (KNT) parts. The total oil and filter wear has again been plotted. It is evident that the differences between the various short cycle gas nitride (KNT) processes are much greater than those between the BNT processes. Variant 5 shows the best results, and is very similar in its wear characteristic to Variant 1, the salt bath high in cyanide/water. With the other KNT variants, wear increases catastrophically sooner or later. With Variant 11 this increase in wear appears in the early stage. Variants 7 and 11 are actually the same process.

Fig. 7 shows the wear characteristics of the plasma nitriding process (PNT), the ion-nitriding variant. In this process the thickness of the compound layer is only 7-12 µm – that is, one-half the thickness of the BNT or KNT layers. According to the manufacturer the thinner layer should guarantee a more porous free layer. With the BNT layers, wear increases at early stages during the main run. Level and rise are similar to those of the least favorable PNT variant. The curves of the different PNT variants show rather similar progressions. The variant with the highest proportion of epsilon phase, that is the variant 2/3 shows the least wear at the end of the main run. The wearing characteristics of the analyzed variant can be compiled in a working sketch and classified with the scope of the test program used here. From the experience gained during vehicle test runs only two variants, that is the BNT Variant 1 and the KNT Variant 5 can be judged as "good." Variants surviving the main run with low wear, and of medium quality, were found to be the BNT variants 2, 3, 4 and 12 and 2/5, as well as the KNT variants 7 and 8. The case-hardened variant is not on the same level, since it showed a very low wear rate during the main run, despite its generally overall high wear level.

Variants that show a rapid rise in wear during the main run must be classified as poor (see Fig. 8). The KNT variants 6 and 11, as well as all PNT variants with the analyzed layer thickness, fall into this category. The wear characteristics of the case-hardened helical gears are basically different from those of the nitrided gears. During the run-in, when the nitrided layers show a wear of approximately 4 milligrams, the case-hardened versions show a wear as high as 80 milligrams, so in the subsequent main run, the case-hardened gears show hardly any wear. At less than 5 milligrams, the main run wear is comparable with that of the good nitrided variant. However, during the overload run one of the two gears shows a catastrophic increase in wear. Case-hardened parts are very sensitive to the addition of sulphur components, for example, zinc thiophosphate.

Damage Analysis

Let us assess the analysis of the damage. All the nitrided helical gears show a similar damage pattern at the end of the test run. There is a pattern of different widths with pittings and more or less large breakouts. The large breakouts frequently go down to the basic material as has been shown by means of spot analysis with copper ammonium chloride. Breakouts may even exist after the run-in. To obtain information on the defect mechanism, test runs were carried out with no activated gear sets of the variants 1, 11 and 12 followed by scanning electron-microscopic examinations and metallographic sections made through the cracks.

Fig. 9 shows a general view of one tooth of each of the three variants. The top illustration records Variant 1, the salt bath high in cyanide/water (BNT), the center represents Variant 12, the salt bath low in cyanide/water (BNT) and the bottom a short cycle gas

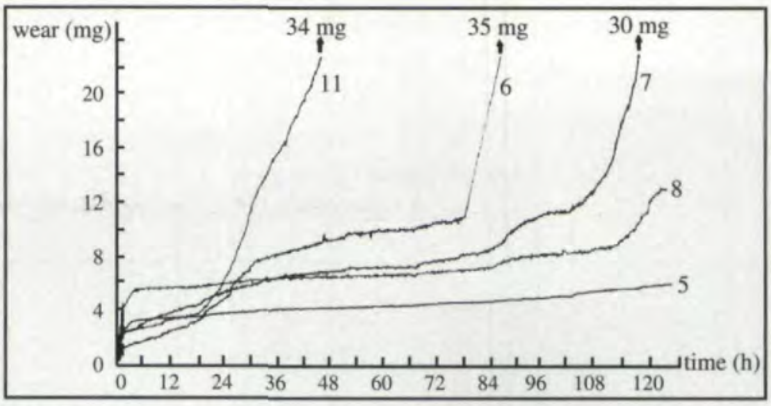

Fig. 6 — Various gas nitriding processes' (KNT) wear characteristics.

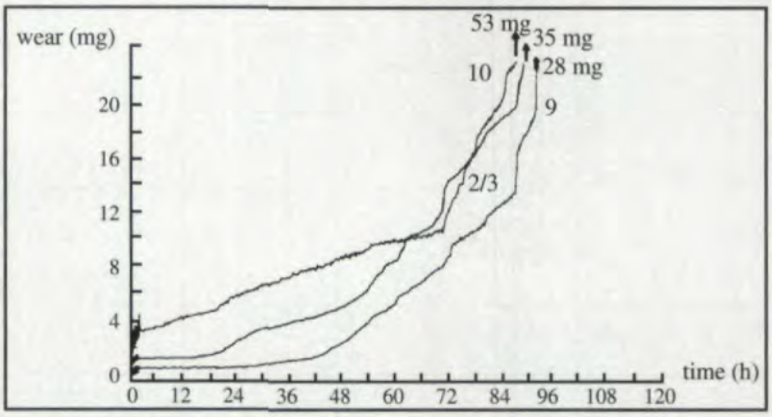

Fig. 7 — Various plasma nitriding processes' (PNT) wear characteristics.

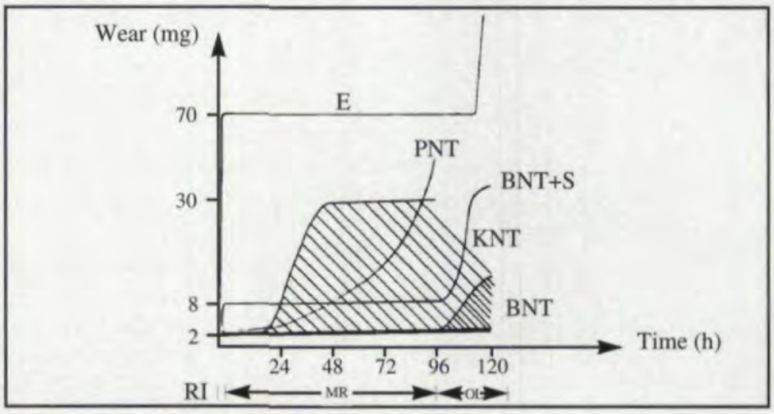

Fig. 8 — Wear characteristics, composite.

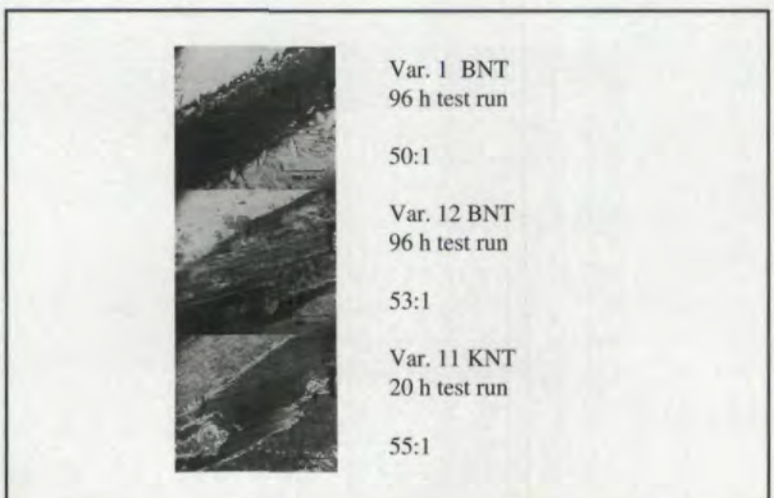

Fig. 9 — General view of wearing zones.

nitrided part. The run-in time was shorter for the gas nitrided gear (KNT) than that for the salt bath nitrided gears (BNT).

Fig. 10 shows this area with greater magnification. On Variant 1 the pittings are completely within the porous zone and only light fracture lines are visible in this area of breakouts. On Variant 12 (Fig. 11) the porous zone has broken out. The destruction extends into the dense portion of the compound layer. The photo of Variant 11 has a magnification of only half that of the other variants, and yet the surface breakouts are of greater magnitude. The damage here extends down to the diffusion zone. The same situation exists on the metallographic section perpendicular to the wear face.

In Fig. 12, photographs of Variant 1 show cracks within the porosity zone. Breakouts occur within this zone. In Fig. 13, photographs of Variant 12 show large areas of subsurface cracking and crack diversification. Similar photographs of Variant 11 (Fig. 14) show pronounced crack diversification, cobblestone-like break outs and cracks in the base material. The cracks generated through a pitting formation are stopped by the extensive porosity zone of Variant 1, in contrast to Variants 11 and 12. The dense layer beneath the porous zone of Variant 1 generates greater resistance to crack propagation than that of Variants 11 and 12.

X-ray diffraction tests were carried out to determine the face composition. The results are shown in Table 2. The readings were taken with molybdenum radiation, allowing for analysis to a depth of approximately 50 µm. Iron-nitride, gamma prime and epsilon iron nitride, as well as amorphous carbo-nitrides, are the major phases occurring over this range. In addition, lines of iron oxides, and, depending upon the thickness of the compound layer, lines of the basic material ferrite, may appear. In practice, the compound layer generally consists of a mixture of epsilon and gamma prime phase in proportions that may vary greatly. However, quantifying this phase mixture is difficult because the phases are not homogeneously distributed in the compound layer, and vary as the depth increases. For a proper interpretation, the compound layer would have to be successively removed.

Since there were two phase examinations performed on the original component, there were two measuring points available for the qualitative analysis. The first was on the tooth of the helical gear, the original layer, and second on the shaft of the helical gear with case removed. The readings taken on the tooth show

Var. 1 BNT
96 h test run

200:1

Var. 12 BNT
96 h test run

210.1

Var. 11 KNT
20 h test run

220:1

Fig. 10 — Details of wearing zones.

Var. 1 BNT
96 h test run

2000:1

Var. 12 BNT
96 h test run

2100:1

Var. 11 KNT
20 h test run

1100:1

Fig. 11 - Details of wearing zones.

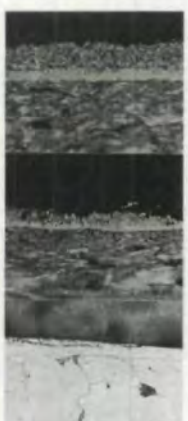

Var. 1 BNT
96 h test run

1000:1

Fig. 12 — Helical gear after test run. Cross section of wearing zone.

very similar diffraction diagrams in practically all cases. Over the analyzed area the layer essentially consists of epsilon phase. Variant 10 is an exception, since it consists of gamma prime mono-phase. Only Variants 2, 3, 9 and 2/3 show distinct gamma prime lines. Variants 4, 7 and 11 show only slight traces. Variants 3 and 11 show distinct iron oxide lines because of the thickness of the compound layer. The alpha iron lines of the basic material are distinctly visible on the PNT layers of Variants 9, 10 and 2/3 only. The readings of the shaft will show more distinct differences between the layers of the different variants. The proportion of the gamma prime phase increases as expected. and is greater in the deeper layers of the compound zone. According to the readings taken, Variants 1, 5, 11 and 12 have the lowest gamma prime proportion.

Variants 1, 11 and 12 were subjected to Auger examinations. They provide the depth profile of the concentration of elements in the compound layer. The Auger examinations were carried out by continuous sputtering of the compound layer using argon ions, rather than on metallographic section perpendicular to the compound layer.

Fig. 15 shows the concentration profiles of the three variants. The nitrogen concentration profiles are similar for all specimens. Major differences are found in the progression of the oxygen and carbon concentration. Variant 11 has a pure iron oxide layer to a depth of 0.6 µm. This is magnetite. However, with a depth of greater than 0.6 µm these specimens have a very low oxygen content, which is distinctly below that of the two BNT variants. Since, as is well known, magnetite forms a brittle layer, this layer may affect the wear characteristics despite the fact that it is relatively thin.

The carbon content of variant 11 is approximately 6-12% and decreases with decreasing nitrogen content towards the matrix material. By contrast, the BNT variants have an increasing carbon content. This effect is particularly striking on the Variant 1, where the carbon content comes up to the level of nitrogen concentration at a depth of approximately 10 µm. Properly speaking, all three variants have, in fact, a carbo-nitride/oxy carbo-nitride layer. The total sum of the oxygen plus carbon plus nitrogen concentrations on Variant 11 is the most stable as

Var. 12 BNT
96 h test run

1000:1

Fig. 13 — Helical gear after test run. Cross section of wearing zone.

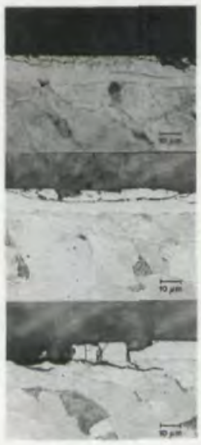

Var. 11 KNT
20 h test run

1000:1

Fig. 14 — Helical gear after test run. Cross section of wearing zone.

Table 2 — X-ray diffraction measurements of compound layer.

Examinations at 2 points on original component

1. on tooth = original surface

2. on shaft = ground surface.

Results:

1. on tooth:	• All variants highly similar • Mainly ε-phase with the exception of Variant 10 • Var. 2, 3, 9 and 2/3 distinctly γ' • Var. 3 and 11 distinctly Fe_3O_4
2. on shaft:	• Difference between different variants, γ' proportion increasing • Variants 1, 5, 11 and 12 have low proportion of γ'-phase

γ'-proportion increases with depth

a function of depth.

Because of the low carbon solubility of the gamma prime phase, the high carbon content of Variant 1 obstructs the formation of the gamma prime. This would also be consistent with the results of the x-ray diffraction tests. The mechanical properties of the epsilon phase, in particular, depend on the level of carbon content in the layer. According to the available literature, the hardness of the epsilon phase decreases rapidly as the proportion of carbon increases. The hardness values of the epsilon phase are generally below those of the gamma prime phase. Hence, it is readily conceivable that an increasing carbon content at depth will cause a continuous transition of the mechanical properties of the compound layer and the mechanical properties of the diffusion layer.

Now, assuming that the ductility (the deforming capability of the layers) is an inverse function of the hardness of the compound zone, then the carbon-containing epsilon compound layer would be the most ductile of all possible layers, that is, the layer with the lowest tendency to brittle crack formation. However, there are also contradictory statements concerning the ductility of the epsilon/gamma prime phase.

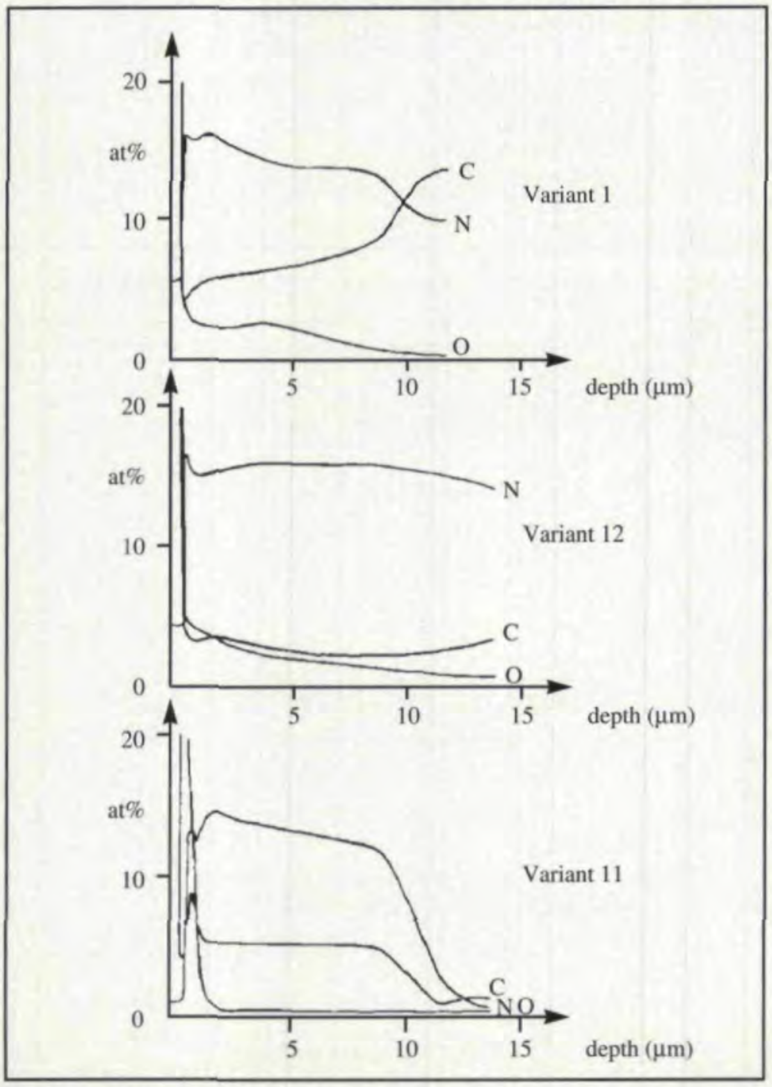

Fig. 15 — Helical gear after test run. Cross section of wearing zone.

Conclusion

In conclusion, we have analyzed the wearing characteristics of nitrided layers made by different processes and have achieved a good classification of the various methods involved. To arrive at a relationship between layer structure and wear characteristics, we have looked more closely into one nitriding variant, each with good, medium and poor wearing characteristics. The nitriding variant with good wear characteristics has the following features: A high proportion of porosity, a very low portion of gamma prime phase (that is, high homogeneity of the compound layer), a rapidly increasing carbon content of the compound layer with increasing depths and a relatively constant oxygen plus nitrogen plus carbon total content over the compound layer. If all these features are present, we believe that pitting is avoided or hindered. The porosity helps to promote good "running-in" characteristics. The homogeneous monoface layer structure and the increasing ductility toward the basic material helps to reduce pitting in the compound layer.

Considering the results of the wear analysis, it would appear that a nitride layer with the properties just mentioned would be easier to obtain by a bath type nitriding than by short cycle gas nitriding. The variants subjected to short cycle gas nitriding revealed greater variation, suggesting that the direction of the treatment parameters plays a more important role. Nevertheless, as has been proved by Variant 5, gaseous short cycle nitriding is quite capable of producing the nitride layer, and has properties equivalent to those obtained in a salt bath. However, our experience tell us that currently the salt bath treatment still has a distinct lead in regard to accuracy of control. ■

Author's note: This research was carried out in cooperation with the companies Robert Bosch and Degussa, within the scope of two projects sponsored by the German Federal Ministry of Research and Technology.